100GHz Electrically Tunable Liquid Crystal Bragg Gratings for Dynamic Optical Networks

F.R. Mahamd Adikan, J.C. Gates, H.E. Major, C.B.E. Gawith, P.G.R. Smith

Optoelectronics Research Centre (ORC), University of Southampton, SO17 1BJ Southampton, United Kingdom

A. Dyadyusha, M. Kaczmarek

School of Physics and Astronomy, University of Southampton, SO17 1BJ Southampton

I.J.G. Sparrow, G.D. Emmerson

Stratophase Ltd, Unit A7, Premier Centre, Premier Way, Romsey, Hampshire SO51 9DG

Abstract: We demonstrate liquid crystal-based integrated optical devices with >140GHz electrical tuning for potential applications in dynamic optical networks. Bragg wavelength tuning covering five 25GHz WDM channel spacings has been achieved with 170V (peak-to-peak) sinusoidal voltages applied across electro-patterned ITO-covered glass electrodes placed 60μm apart. This tunability range was limited only by the initial grating strength and supply voltage level. We also observed two distinct threshold behaviors that manifest during increase of supply voltage, resulting in a hysteresis in the tuning curve for both TE and TM input light.

OCIS codes: (130.0130) Integrated optics; (130.3120) Integrated optics devices; (230.0230) Optical devices; (230.2090) Electro-optical devices

Introduction: Increasingly fast and high density wavelength division multiplexing (WDM) networks place stringent requirements on channel spacing and integrity. With 25GHz channel spacings becoming more commonplace, the ability to dynamically add and drop channel information will increase network scalability and reach while keeping operational

expenditures manageable. In view of this, one field that is currently receiving a great deal of attention is the development of dynamic, reconfigurable integrated optical devices and components in silica-on-silicon, including arrayed waveguides and MEMS [1]. While limited wavelength or frequency filtering is often added via a planar Bragg grating, developing the ability to tune the peak reflection wavelength over several standard channel spacings could prove to be one of the key enablers in realizing an all-optical dynamic network.

To date, very little has been reported on electrically-tunable planar Bragg gratings given the potentially superior response time over their more commonly used temperature-tuned counterparts. Such electrically tunable devices work on the principle of shifting the Bragg wavelength by modifying the effective refractive index of a waveguide in a multilayer substrate, as described by the equation $\lambda_B=2\Lambda n_{eff}$ (where λ_B is the Bragg centre wavelength, Λ is the grating period, and n_{eff} is the effective index of the waveguide). One potential route to achieve this is by overlaying the grating structure with a liquid crystal. Many liquid crystals display refractive index anisotropy due to their molecular structure and orientation that can be manipulated using an electric field. Changes to the liquid crystal index subsequently alter the effective index of the waveguide, leading to Bragg wavelength shift. Using this approach, Sparrow et al [2] have previously described 35GHz electrically tunable planar Bragg gratings in silica-on-silicon at 1560nm using an 80Vpp (peak-to-peak) square wave with 250µm-spaced aluminum electrodes. Theoretical analysis of devices utilizing similar concepts for switching and tunability can be found in [3, 4] for example.

In this paper, we demonstrate electrically tunable first order Bragg gratings via liquid crystal index modification with a maximum tunability of 141 GHz at 1562 nm and 114 GHz at 1561.8nm for transverse magnetic (TM) and transverse electric (TE) polarized input light respectively. Electro-patterned ITO-coated glass was used to provide a local electrode structure as opposed to conventional metal deposition. The tunability range was achieved with 170Vpp supply voltage at 1 kHz and is limited by the initial grating reflection strength (~17 dB with respect to noise level) and the supply voltage level. We also observed two

distinct threshold behaviors which manifest only during increase of supply voltage, giving hysteresis in the tuning curve.

Fabrication of Gratings and Device Assembly: The samples used for this experiment were 3-layer silica-on-silicon with germanium doped core layer to allow for photosensitivity to 244 nm UV radiation. Diced and polished samples were hydrogen loaded under pressure at 120 bar to increase photosensitivity and waveguides and Bragg gratings were defined using Direct Grating Writing, a technique which uses an interference pattern generated by crossed UV beams to simultaneously define channel waveguides and grating structures, as described in [5]. After UV writing the overclad layer covering the 2-mm-long Bragg gratings was removed using hydrofluoric acid wet etching. The electrodes were prepared by electro-patterning (electrically scribing) through a piece of single sided Indium Tin Oxide (ITO) coated glass. The spacing between the electrodes is estimated to be ~60 µm and the patterned glass was then cut to match the dimensions of the UV-written sample. Homeotropic alignment of the liquid crystal molecules was achieved by applying a thin layer of surfactant (Merck liquicoat ZLI-3334 0.2% solution in ethanol) in the etched area and on the ITO electrodes and both were then baked at 180 ºC for one hour to ensure good surfactant adhesion. The ITO electrodes were then attached to the top of the sample using supporting glass spacers to allow sample movement for aligning the etched waveguide with the electrodes. Merck 18523 liquid crystal was then inserted into the etched window under vacuum. This liquid crystal displays estimated extraordinary and ordinary refractive index values of 1.49 (n_e) and 1.44 (n_o) at 1550nm respectively [6]. The assembled device is schematically shown in Figure 1.

The electrodes were aligned to the waveguide prior to each experimental run by launching a HeNe laser into the waveguide and observing the scattering from the exposed part of the waveguide. The electrodes were then carefully aligned to this scattering ‘footprint’. Light from an amplified spontaneous emission source (wavelength range between 1520 to 1565nm) was polarized and launched into the waveguide via butt-coupling with a polarization

maintaining fiber tipped with index matching oil. The reflected signal was assessed using a commercial optical spectrum analyzer. Computer-based software was used to control the voltage level supplied to the device and to obtain various data including the grating spectrum for each voltage level set and the centre wavelength shift with respect to the initial (zero voltage) condition. A Gaussian Levenberg-Marquardt (Lev-Mar) curve fitting function was employed in the control program to determine the peak Bragg wavelength.

Results and Discussions: Figure 2 shows the absolute Bragg wavelength shift curve of the device for both TM and TE launched input light. For TM input, the curve exhibits 1.15 nm (141 GHz) Bragg wavelength shift over 170Vpp supply voltage and 0.93 nm (114GHz) shift was recorded for the TE case. Both curves display hysteresis between points A and B. Repeat measurements were conducted over a period of several weeks to validate the hysteretic behavior. Inset (i) shows a typical tuning curve with increase in voltage whereas inset (ii) shows the curve with decreasing voltage. It was observed in all measurements that the curves for increasing voltage exhibit two distinct points where the tuning gradient increases significantly. We discovered that for both TM and TE inputs the primary threshold is observed at ~18±4Vpp supply voltage, whereas the secondary threshold point seems to appear over a wider margin, around 57±10Vpp. These threshold behaviors are not seen in the decreasing voltage curve where a more linear behavior is obtained. We believe that the primary threshold is the point where the applied electric field is large enough to overcome interactions of liquid crystal molecules with surfaces and elastic forces. The origin of the secondary threshold is not clear, but is likely due to the multi-domain structure of liquid crystals created in the confined area of the etched window and their interactions with an applied field, creating disclination along a particular axis. Unexpectedly, both TE and TM show reduced effective index for higher voltages. This cannot be explained by simple geometric arguments and will be the subject of future studies.

Figure 3 shows that grating spectra measurements at the two threshold points have no noticeable difference in terms of grating strength and shape. This further supports the

argument that the effect is physical in nature and is related to the liquid crystal overlay behavior under applied electric field.

The overall tuning range of our devices was limited by the effective refractive index of the host channel waveguide and original (no applied voltage) reflection strength of the incorporated Bragg grating. This effect is due to the refractive index of the liquid crystal, which is larger than that of the waveguide and thus causes loss of modal confinement and a weaker grating response while the device is operated at higher voltages. As such, we believe that by implementing stronger waveguides with a narrower Bragg grating reflection an even larger tuning range will be attainable. In addition, our power supply system is currently limited to 170Vpp before the advent of signal clipping and we also believe that further tuning is achievable with higher voltage levels.

Conclusions: We have demonstrated an electrically tunable first order Bragg grating via liquid crystal index modification with a maximum tunability of 141GHz at 1562nm (TM polarized) and 114GHZ at 1561.8nm (TE polarized) using electro-patterned ITO-coated glass electrodes. The 141GHz tuning range effectively covers up to five 25GHz WDM channel spacings and work to expand this limit by optimizing grating strength, modal loss, supply voltage, and crystal behaviour are planned. Future developments towards a cascaded architecture of such integrated liquid crystal devices operating at different Bragg wavelengths could pave the way towards true colorless add/drop modules for dynamic dense optical networks.

References

[1] D. T. Neilson, C. R. Doerr, D. M. Marom, R. Ryf, and M. P. Earnshaw, Bell Labs Tech. J., **11**, 105 (2006).

[2] I. J. G. Sparrow, G. D. Emmerson, P. G. R. Smith, M. Kaczmarek, and A. Dyadyusha, "35 GHz tunable planar Bragg grating using nematic liquid crystal overlay," in *European Conference on Integrated Optics* (2005), paper ThP01.

[3] L. Sirleto, G. Coppola, G. Breglio, G. Abbate, G. C. Righini, and J. M. Oton, Opt. Eng., **41**, 2890 (2002).

[4] R. Asquini, A. Fratalocchi, A. D'Alessandro, and G. Assanto, Appl. Optics, **44**, 4136 (2005).

[5] G. D. Emmerson, S. P. Watts, C. B. E. Gawith, V. Albanis, M. Ibsen, R. B. Williams, and P. G. R. Smith, Electron. Lett., **38**, 1531 (2002).

[6] R.-P. Pan, S.-R. Liou, and C.-K. Lin, Jpn. J. Appl. Phys. 1, **34**, 6410 (1995).

FIGURE CAPTIONS

Figure 1: A schematic representation of the assembled device showing the liquid crystal overlay in between the electro-patterned ITO electrodes and the waveguide containing Bragg gratings. Overclad, core, and underclad thickness are ~ 20, 5 and 20 µm respectively with a waveguide width of ~ 5 µm. **(Color online)**

Figure 2: Absolute device tuning curves for both TM and TE polarized light showing hysteresis between points A and B. The insets show the same curves for increasing (arrow pointing upwards) and decreasing (arrow pointing downwards) voltages. In inset (i), the circles numbered 1 and 2 shows the two threshold points at ~22V and ~57V respectively. **(Color online)**

Figure 3: Grating reflection spectra at the two threshold points. The primary threshold for this case is between 22-23Vpp whereas the secondary threshold point is between 46-48Vpp. No noticeable difference in terms of grating reflection spectral shape and strength is observed at these transitions. Lev-Mar theoretical profiles are also shown on two of the graphs.
(Color online)

Figure 1

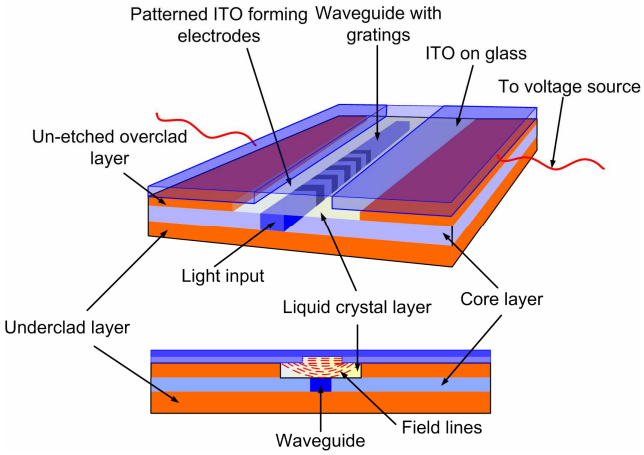

(Color online)

Figure 2

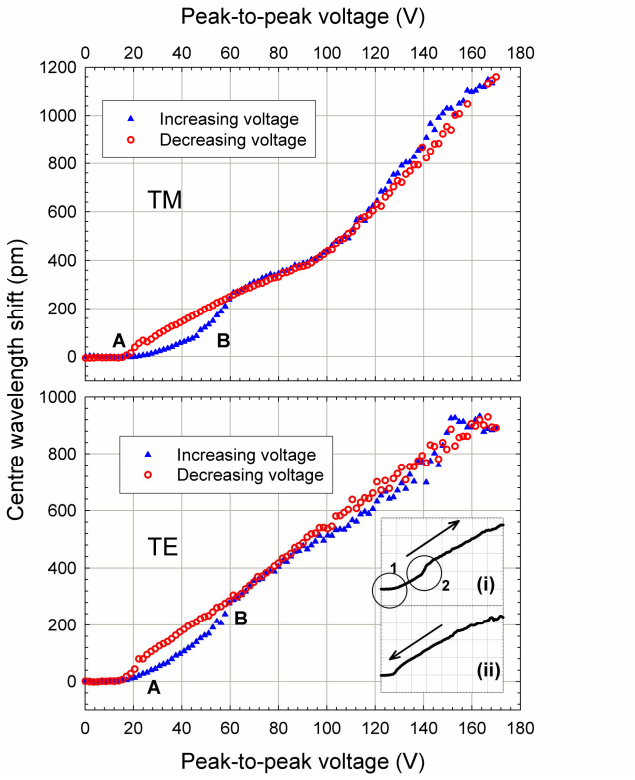

(Color online)

Figure 3

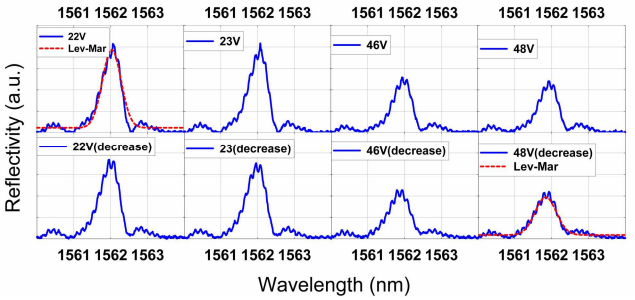

(Color online)